Title: Multi-Connection Pattern Analysis: Decoding the Representational Content of Neural Communication

Authors: Yuanning Li[1,2,3*] and Avniel Singh Ghuman[1,2,3]

Affiliations:
[1]Center for the Neural Basis of Cognition.
[2]Program in Neural Computation, Carnegie Mellon University and University of Pittsburgh.
[3]University of Pittsburgh, Department of Neurological Surgery.

Classification:
Biological Sciences (Neuroscience; Psychological and Cognitive Sciences)

*Correspondence to:

Yuanning Li
S906 Scaife Hall
3550 Terrace Street
Pittsburgh, PA 15261
ynli@cmu.edu

Abstract

What information is represented in distributed brain circuit interactions is unknown due to the lack of multivariate methods for decoding the representational content of interregional neural communication. Here we present Multi-Connection Pattern Analysis (MCPA), which probes the nature of the representational space contained in the multivariate functional connectivity pattern between neural populations. MCPA works by learning mappings between the activity patterns of the populations as a factor of the information being processed. These maps are used to predict the activity from one neural population based on the activity from the other population. Successful MCPA-based decoding indicates the involvement of distributed computational processing and provides a framework for probing the representational structure of the interaction. Simulations demonstrate the efficacy of MCPA in realistic circumstances. Applying MCPA to fMRI data shows that interactions between visual cortex regions are sensitive to information that distinguishes individual natural images, suggesting that image individuation occurs through interactive computation across the visual processing network. MCPA-based representational similarity analyses (RSA) are used to test hypotheses regarding information transformation between regions of the visual processing network. These results support models of error coding in interactions among regions of the network. Further RSA analyses relate the non-linear information transformation operations between layers of a computational model (HMAX) of visual processing to the information transformation between regions of the visual processing network. Thus, MCPA can be used to assess the information represented in the coupled activity of

interacting neural circuits and probe the underlying principles of information

transformation between regions.

Significance Statement

Information is represented in the brain by the coordinated activity of neurons at both the regional level and the level of large-scale, distributed networks. Multivariate methods from machine learning have advanced our understanding of the representational structure of local information coding, but the nature of distributed information representation remains unknown. Here we present a novel method that integrates multivariate connectivity analysis with machine learning classification techniques that can be used to decode the representational structure of neural interactions. This method is used to probe the representational structure of the interaction between regions of visual cortex and relate this structure to a computational model of visual processing. Thus, this work provides a framework to assess the representational content of circuit-level processing.

\body

Introduction

Since at least the seminal studies of Hubel and Wiesel (1) the computational role that neurons and neural populations play in processing has defined, and has been defined by, how they are tuned to represent information. The classical approach to address this question has been to determine how the activity recorded from different neurons or neural populations varies in response to parametric changes of the information being processed. Single unit studies have revealed tuning curves for neurons from different areas in the visual system responsive to features ranging from the orientation of a line, shapes, and even high level properties such as properties of the face (1-3). Multivariate methods, especially pattern classification methods from modern statistics and machine learning, such as multivariate pattern analysis (MVPA), have gained popularity in recent years and have been used to study neural population tuning and the information represented via population coding in neuroimaging and multiunit activity (4-11). These methods allow one to go beyond examining involvement in a particular neural process by probing the nature of the representational space contained in the pattern of population activity (12-14).

Neural populations do not act in isolation, rather the brain is highly interconnected and cognitive processes occur through the interaction of multiple populations. Indeed, many models of neural processing suggest that information is not represented solely in the activity of local neural populations, but rather at the level of recurrent interactions between regions (15-17). However previous studies only focused on the information representation within a specific population (3, 4, 10, 11, 18, 19), as no

current multivariate methods allow one to directly assess what information is represented in the pattern of functional connections between distinct and interacting neural populations. Such a method would allow one to assess the content and organization of the information represented in the neural interaction. Thus, it remains unknown whether functional connections passively transfer information between encapsulated modules (20) or whether these interactions play an active computational role in processing.

Univariate methods that go beyond assessing the degree of coupling between to populations to assess changes in the relationship between the activity as a factor of condition also examine active communication between regions. For example the psychophysiological interactions (PPI; (21)) and dynamic causal modeling methods (22) are sensitive to active interregional communication. However, when compared with univariate methods, it has been noted that multivariate methods allow for "more sensitive detection of cognitive states," "relating brain activity to behavior on a trial-by-trial basis," and "characterizing the structure of the neural code" (23). Thus, a multivariate pattern analysis method for functional connectivity analysis is critical for decoding the representational structure of interregional interactions.

In this paper, we introduce a multivariate analysis algorithm combining functional connectivity and pattern recognition analyses that we term Multi-Connection Pattern Analysis (MCPA). MCPA works by learning the discriminant information represented in the shared activity between distinct neural populations by combining multivariate correlational methods with pattern classification techniques from machine learning in a novel way. Much the way that MVPA goes beyond a t-test or ANOVA by building a multivariate model of local activity that is then used for single-trial prediction and

classification, MCPA goes beyond PPI by building a multivariate connectivity model that is then used for single-trial prediction and classification. This single-trial prediction and classification makes MCPA distinct from previous connectivity approaches that only statistically test the absolute or relative functional connectivity between two populations (24-28) and allows for a detailed probe of the representational structure of the interaction.

The MCPA method consists of an integrated process of learning connectivity maps based on the pattern of coupled activity between two populations A and B conditioned on the stimulus information and using these maps to classify the information representation in shared activity between A and B in test data. The rationale for MCPA is that if the activity in one area can be predicted based on the activity in the other area and the mapping that allows for this prediction is sensitive to the information being processed, then this suggests that the areas are communicating with one another and the communication pattern encodes the information being processed. Thus, MCPA simultaneously asks two questions: 1) Are the multivariate patterns of activity from two neural populations correlated? (i.e. is there functional connectivity?) and 2) Does the connectivity pattern adaptively change based on the information being processed? This is operationalized by learning a connectivity map that maximizes the multivariate correlation between the activities of the two populations in each condition. This map can be thought of like the regression weights that transform the activity pattern in area A to the activity pattern in area B (properly termed "canonical coefficients" because a canonical correlation analysis [CCA] is used to learn the map). These maps are then used to generate the predictions as part of the classification algorithm. Specifically, a prediction of the activity pattern in one region is generated for each condition based on

the activity pattern in the other region projected through each mapping. Single trial

classification is achieved by comparing these predicted activity patterns with the true

activity pattern (see Figure 1 for illustration). With MCPA single trial classification based

on multivariate functional connectivity patterns is achieved allowing the nature of the

representational space of the interaction to be probed.

We present a number of simulations to validate MCPA for a realistic range of

signal-to-noise ratios (SNR) and to show that MCPA is insensitive to local information

processing. We apply MCPA to examine the inter-regional representation for natural

visual stimuli in visual cortex using functional magnetic resonance imaging (fMRI) data.

Specifically, we show that the interactions between regions of the visual stream (V1, V2,

V3, V4, and LO) are sensitive to information about individual natural images. We

combine MCPA with representational similarity analysis to demonstrate that MCPA can

be used to evaluate computational models and make inferences regarding the underlying

neural mechanism of information transferring. These results demonstrate that MCPA can

be used to probe the nature of representational space resulting from processing distributed

across neural regions.

Results

Simulations

We used simulations to test and verify the performance and properties of MCPA on synthetic data. Specifically, synthetic data generated based on real fMRI data representing neural activity of two distinct populations and the information represented in the interaction between those populations was manipulated to construct different testing conditions.

In the first simulation, we evaluated the ability of MCPA to detect information represented in the functional connectivity pattern when it was present as a factor of the SNR and the number of dimensions of the data. The mean and standard error of the sensitivity index (d') from 100 simulation runs for each particular setup (dimensionality and SNR) are shown in Figure 2a. The performance of the MCPA classifier increased when SNR or effective dimensionality increased. Classification accuracy saturated to the maximum when SNR and number of dimensions were high enough (SNR > 5 dB, dimensionality > 10). The performance of MCPA was significantly higher than chance (p < 0.01, permutation test) for SNRs above -5 dB for all cases where the dimensionality was higher than 2, when the pattern of the multivariate mapping between the activity was changed between conditions. It is notable that significant MCPA classification was seen despite there being no local information present in either of the two simulated populations (p > 0.1 for all cases using MVPA).

The first control simulation was designed to confirm that when two unconnected populations both carry local discriminant information, MCPA would not be sensitive to that piece of information. As shown in Figure 2b, MCPA did not show any significant

classification accuracy above chance ($d' = 0$) as k changed. On the other hand, the

MVPA classifier that only took the data from local activity showed significant

classification accuracy above chance level and the performance increased as local

discriminant information increased.

The second control simulation was designed to test if MCPA would be insensitive

to changes in local discriminant information when there was constant information coded

in neural communication. Local discriminant information was injected into the

populations by varying the ratio of the standard deviation (k) between the two conditions.

When MVPA was applied to the local activity, increasing classification accuracy was

seen as k became larger (Figure 2c). This result confirmed that discriminant information

was indeed encoded in the local activity in the simulation. On the other hand, the

performance of MCPA did not change with the level of local discriminant information (d'

stayed around 1.65 for all cases), demonstrating that MCPA is only sensitive to changes

in information contained in neural interactions.

The final control simulation tested whether MCPA is simply sensitive to the

presence of functional connectivity between two populations *per se* or is only sensitive to

the whether the functional connectivity contains discriminant information. Specifically,

are local discriminant information in two populations, and a correlation between their

activity, sufficient for MCPA decoding? It should not be considering that MCPA requires

that the pattern of the mapping between the populations to change as a factor of the

information being processed (see Figure 1). For example, the local activity in either or

both populations could code for the information being processed, but the mapping

between the activity in each region could be constant and insensitive to the changes in

conditions, e.g. the CCA coefficients could be the same. This would be the case if each population was an informationally encapsulated module where information transfer occurs in the same way regardless of the stimulus being processed or cognitive state. In this case, one would not want to infer that distributed processing was taking place because the nature of the interregional communication is not sensitive to the computation being performed (e.g. the information transfer is passive, rather than reflecting distributed computational processing) and all of the information processing is done locally in each population. The final control simulation was designed to assess whether MCPA is sensitive to the case where two populations communicate, but in a way that would not imply distributed computational processing. Specifically, neural activity in areas A and B were simulated such that local discrimination was possible in each population and the activity of the two populations was correlated, but the interaction between them was invariant to the information being processed. Figure 2d shows that in this case MCPA did not classify the activity above chance, despite significant correlation between the regions and significant local classification (MVPA). Thus, functional connectivity between the populations is a necessary, but not sufficient, condition for MCPA decoding. Therefore, MCPA is only sensitive to the case where the mapping itself changes with respect to the information being processed, which is a test of the presence of distributed neural computation.

Single image classification of visual cortex interactions using MCPA

To assess its performance on real neural data, MCPA was applied to Blood-oxygen-level-dependent (BOLD) fMRI measurements of human occipital visual areas, in two subjects (Subject 1 and Subject 2) during passive viewing of 13 repetitions of 120

natural images (29-31). MCPA was used for single-trial classification of these images for the interactions between V1-V2, V2-V3, V3-V4, and V4-lateral occipital (LO) cortex (e.g. 4 total region pairs * 2 subjects; see Figure 5 of Naselaris et al. (31) for depictions of these regions in these subjects). Across the 8 pairs of regions the mean sensitivity index (d') of the single trial classification was 0.405 (SD = 0.094), with all of the pairs showing significant classification at $p < 0.05$ corrected for multiple comparisons. In both subjects, MCPA classification accuracy declined going up the classic visual hierarchy. For Subject 1, the classification accuracies (d') were 0.451 (V1-V2), 0.432 (V2-V3), 0.403 (V3-V4), and 0.333 (V4-LO); for Subject 2, the classification accuracies (d') were 0.563 (V1-V2), 0.469 (V2-V3), 0.317 (V3-V4), and 0.274 (V4-LO).

   To assess whether the information represented in the between region interactions reflected a distinct computational process or merely reflected the representation in either of the individual areas, a representational similarity analysis (RSA) was performed. To increase our power, we performed this RSA at the category level (animals, buildings, humans, natural scenes, and textures) based on classification accuracy rather than the single image level because the dataset contained many more repetitions per category than per image (Figure 3). This yielded a total of 16 correlations (8 MCPA-based matrices correlated with each of the two regions that contribute to each MCPA). 13 out of the 16 correlations were negative, many showing large negative correlation coefficients (see Table 1 for details, mean Spearman's rho = -0.415, SD = 0.364). In other words, categories that were relatively easy to decode based on the activity within regions using MVPA were relatively more difficult to decode based on the shared activity between that region and the other regions in the visual stream using MCPA and vice versa (Figure 3).

This negative correlation suggests that the communication between regions represents information that has not been explained aspects by local computational processes.

Comparing MCPA to PPI

To demonstrate the dominance of MCPA over classical univariate methods, we applied PPI to the same data to analyze categorical effective analysis between neighboring areas. As a comparison, 80 different pairs of categories (10 pairs of categories * 4 pairs of regions * 2 subjects) were analyzed using both PPI and MCPA. 4/80 PPI results were significant with $p < 0.05$ (uncorrected), while 13/80 MCPA results were significant with $p < 0.05$ (uncorrected). As a result, with a binomial test, PPI did not show significant result on 80 samples (4/80, $p = 0.5$), while MCPA was significantly above chance level (13/80, $p < 0.001$).

Using MCPA-based RSA to test models of between-area information transformation

One important application of MCPA is to evaluate models and test theoretical hypotheses regarding the computational operation underlying how representations are transformed from one region to another. MCPA-based RSA can be used to compare the representational space derived from the interaction between brain regions to representational spaces derived from the transformation of representations in computational models. To illustrate this we compare the representational space for natural images in the same fMRI dataset described above to the representational space derived from the transformation between layers of the HMAX model of the visual processing stream (32, 33). HMAX has four layers going from S1 to C1 to S2 to C2 along the hierarchy. The transformation of the representation between S1 and C1 (S1-C1 transformation) occurs through a local, non-linear max-pooling operation and the

transformation between S2 and C2 (S2-C2 transformation) occurs through a more global non-linear max-pooling operation. We compared the representational dissimilarity matrices (RDMs) derived from these HMAX transformations to the RDMs derived from MCPA between V1-V2, V2-V3, V3-V4, and V4-LO. The transformation between C1 and S2 occurs through a passive filtering that does not give rise to an RDM because the transformation is effectively the same across all C1 representations.

As shown in Figure 4, we found that the RDM derived from the S1-C1 transformation in HMAX correlates with the V2-V3 RDM based upon MCPA of the fMRI data (mean Spearman's rho = 0.053, $p < 0.05$, permutation test). Furthermore, the S1-C1 correlation to V2-V3 was significantly greater ($p < 0.05$, permutation test) than the S2-C2 correlation to V2-V3. The RDM derived from the S2-C2 transformation in HMAX correlates with the V4-LO RDM based upon MCPA of the fMRI data (mean Spearman's rho = 0.112, $p < 0.001$, permutation test). Furthermore, the S2-C2 correlation to V4-LO was significantly greater ($p < 0.01$, permutation test) than the S1-C1 correlation to V4-LO. Additionally, none of the individual layers in HMAX showed a consistent significant correlation with the connectivity-based RDM from MCPA. Taken together, these results suggest that the interaction between the lower layers of the neural visual hierarchy reflects an operation more like the operation between the lower layers of the model of the visual hierarchy than between higher layers of the model. Furthermore, the interaction between higher layers of the neural visual hierarchy reflects an operation more like the operation between higher layers of the model than between lower layers of the model.

Discussion

This paper presents a novel method to assess the information represented in the patterns of interactions between two neural populations. MCPA works by learning the mapping between the activity patterns from the populations from a training data set, and then classifying the neural communication pattern using these maps in a test data set. Simulated data demonstrated that MCPA was sensitive to information represented in neural interaction for realistic SNR ranges. Furthermore, MCPA is only sensitive to the discriminant information represented through different patterns of interactions irrespective of the information encoded in the local populations. Applying this method to fMRI data demonstrated that the multivariate connectivity patterns between areas along the visual stream represent information about individual natural images. MCPA-based RSA showed that, at the category level, the representational structure of the interaction between regions is negatively correlated to the structure within each region. Finally, MCPA was used to test hypotheses from the HMAX model regarding the computational operation that transforms the representation between regions along the visual processing pathway.

It is worth noting that significant discrimination within each population and significant functional connectivity between them is not sufficient to produce MCPA and indeed local classification within each population is not even necessary (Figures 2d and 2a respectively). MCPA requires the pattern of connectivity between the two populations to vary across the different conditions. As an example, if the two populations interact, but the interaction behaves like a passive filter, mapping the activity between the populations in a similar way in all conditions, MCPA would not be sensitive to the interaction

because the mapping does not change (Figure 2d). Instead, MCPA is more akin to testing

for adaptive filtering or distributed, interactive computation where the nature of the

interaction changes depending on the information that is being processed. Recent studies

demonstrate that neural populations in perceptual areas alter their response properties

based on context, task demands, etc. (34). These modulations of response properties

suggest that lateral and long-distance interactions are adaptive and dynamic processes

responsive to the type of information being processed. MCPA provides a platform for

examining the role of interregional connectivity patterns in this adaptive process. Indeed,

MCPA can be interpreted as testing whether distributed computational "work" is being

done in the interaction between the two populations (21) and the interaction does not just

reflect a passive relay of information between two encapsulated modules (20).

In addition to allowing one to infer whether distributed computational work is

being done in service of information processing, MCPA provides a platform for assessing

its representational structure. Much as MVPA has been used in representational similarity

analyses to measure the structure of the representational space at the level local neural

populations (12, 13, 35), MCPA can be used to measure the structure of the

representational space at the level of network interactions. Specifically, the

representational geometry of the interaction can be mapped in terms of the similarity

among the multivariate functional connectivity patterns corresponding to the brain states

associated with varying input information. The representational structure can be

compared to behavioral measures of the structure to make brain-behavior inferences and

assess what aspects of behavior a neural interaction contributes to. It can also be

compared to models of the structure to test theoretical hypotheses regarding the

computational role of the neural interaction (35, 36).

These two properties of MCPA, 1) being able to assess distributed computational

processing rather than just whether or not areas are communicating and 2) being able to

determine the representational structure of the information being processed, set MCPA

apart from previously proposed functional connectivity methods. In these previous

methods the functional connectivity calculation is performed separately from the

classification calculation. Specifically, either functional connectivity is first calculated

using standard methods, then a model is built on the population of connectivity values

and this model is tested using classification approaches (24, 26-28, 37) or the model is

first built on the activity in each region and tested using classification approaches and the

classification performance is correlated (13, 38). These methods are very useful for

assessing how differences large-scale patterns of connectivity relate to individual subject

characteristics (e.g. connectome fingerprinting) in the first case and comparing the

representational structure between regions in the second case. In contrast, in MCPA the

model is the connectivity map and classification is done to directly test the information

contained in these maps. The separation of the connectivity and classification calculations

in other approaches precludes being able to assess distributed computational processes

because these methods are sensitive to passive information exchange between

encapsulated modules, as described above, and thus conflate passive and active

communication. Critically, they do not specifically probe how connectivity patterns

change as a factor of condition or state, as is required to efficiently perform the

representational similarity analysis in a practical manner and decode how the information

processed in the interaction is encoded and organized. As a concrete example, these previous methods would not be able to compare the representational structure of the neural interaction between regions to the structure from a computational model, as was done here with fMRI.

MCPA can be roughly considered a multivariate extension of PPI with the addition of a prediction and classification framework. Compared to PPI, which is univariate, MCPA allows one to exploit the multivariate space of interaction patterns. As a result, MCPA is sensitive to aspects of information coded in interregional interactions that PPI cannot detect (23), for example in event-related fMRI designs where PPI is known to lack statistical power (39). Indeed, in the fMRI data presented here, PPI was no better than chance in detecting interregional interactions at the visual category level, whereas MCPA was significantly better than chance. Much the way MVPA allows one to go beyond ANOVAs/t-tests in a single area/population (e.g. single trial classification, RSA, complex model testing), MCPA allows one to go beyond PPI and do these types of analyses at the level of the shared activity between regions.

An important potential use for MCPA is that a MCPA-based RSA can help inform models of how representations are transformed between neural populations along a processing pathway (14). An increasingly successful approach for evaluating and developing computational models of neural processing is by assessing the similarity between the representations implied by the models to the one measured in the brain (36), e.g. MVPA-based RSA. By comparing the representational space in models to the neural representation, one can assess how well these models approximate the neural representation in both absolute and relative terms. Much the way MVPA-based RSA

analyses have been used to examine these models at the level of individual brain regions

(36), RSA analyses can be used to assess how well the representation inferred by these

models' transfer functions fit the representation measured in the brain using MCPA. The

MCPA-based RSA analysis presented here relating the representational space derived

from the interaction between regions of the visual processing stream to the transformation

operations in HMAX is a concrete example of how MCPA can be used to test models of

how representations are transformed between regions. This example also helps illustrate

the underlying hypothesis being tested by MCPA: that there is a non-constant function

that relates how the transformation of the activity between regions changes with respect

to the experimental condition. The existence of this non-constant function is what is

meant by active processing and distributed computational work. By comparing the

MCPA-based representational space to models of this function, we can gain insight into

what this transformation function might be. For example, in the case of the S1-C1

transformation HMAX, this function is a local, non-linear max-pooling operation and in

the case of the S2-C2 operation it is a more global, non-linear max-pooling operation (32).

Furthermore, this is why MCPA could not be compared to the transformation between the

C1 and S2 layers of the HMAX model because the transformation between those layers is

a passive filter operation, e.g. a trivial, constant function relating the between layer

transformation to the stimulus condition. This example suggests one mechanism by

which a network with fixed structural connectivity can give rise to active communication,

namely through a non-linear transformation operation. In addition to testing specific

hypothesis-driven transformation operations, such as the ones in HMAX, more data-

driven models of the transformation operations, such as ones in deep neural network models (40), could also be tested using the MCPA-based RSA approach.

The specific instantiation of MCPA presented here treats connectivity as a bi-directional linear mapping between two populations. However, the MCPA framework could be easily generalized into more complicated cases. For example, instead of using correlation-based methods like CCA, other directed functional connectivity algorithms, such as Granger causality based on an autoregressive framework, potentially using partial CCA for the time-lagged autoregressive step, could be used to examine directional interactions. This would allow one to examine time-lagged multivariate connectivity patterns to infer directionality. Additionally, kernel methods, such as kernel CCA(41), or deep learning methods, such as deep CCA(42), could be applied to account for non-linear interactions. Another possible and more general framework would be to use non-parametric functional regression method to build a functional mapping between the two multidimensional spaces in the two populations. MCPA can also be expanded to look at network-level representation by implementing the multiset canonical correlation analysis, wherein the cross-correlation among multiple sets of activity patterns from different brain areas is calculated (43). MCPA could be used with a dual searchlight approach to examine whole brain communication (44). Also, MCPA could be adapted by optimizing the CCA to find the connectivity maps that uniquely describe, or at least best separate, the conditions of interest. Furthermore, both with and without these modification, the framework of MCPA may have a number of applications outside of assessing the representational content of functional interactions in the brain, such as detecting the presence of distributed processing on a computer network, or examining genetic or

proteomic interactions. MCPA is used here with fMRI BOLD signals, but it can be applied to nearly any neural recording modality, including scalp or intracranial electroencephalography, magnetoencephalography, multiunit firing patterns, single unit firing patterns, spike-field coherence patterns, to assess the information processed by cross-frequency coupling, etc.

The MCPA results from visual cortex show that the representational space derived from MCPA was negatively correlated to the representational space derived from MVPA from either of the local populations. This inverse relationship is consistent with the idea that the communication between regions represents information that has not been explained by local computational processes. This is supportive of models that propose coding for error propagation across the visual processing network (45) or Bayesian models that suggest that visual processing occurs through iterative prediction-verification processing (16). Indeed, some implementations of this class of models, interactions between regions are thought to code for prediction errors (46), which would predict the negative correlation seen here. More generally, these results suggest another mechanism through which a network with fixed structural connectivity can give rise to active communication, namely through local or interregional recurrent interactions. With the strong caveat that these results require replication in more subjects and assessment with paradigms designed to directly test these hypotheses, this negative correlation is consistent with the hypothesis that neural interactions code for information not resolved in local computational processes.

Additional RSA analysis suggests that the transformation between lower layers of HMAX correlates with the transformation between lower layers of the ventral visual

stream and the transformation between higher layers of HMAX correlates with the actual transformation between higher layers of the ventral visual stream. One question is how the representation between regions of the visual processing stream can correspond to both prediction error and the HMAX max pooling operation, as found in the two RSA analyses. One possibility is that these two operations occur at different times during visual processing, which are mixed together due to the low temporal resolution of fMRI. Indeed, HMAX is designed to model the initial feedforward sweep of visual information and the error coding is thought to occur through later recurrent and feedback processing. More broadly, the MCPA results suggest that the computational work done in service of visual processing occurs not only on the local level, but also at the level of distributed brain circuits.

Conclusion

Previously, multivariate pattern analysis methods have been used to analyze the sensitivity to information within a certain area and functional connectivity methods have been used to assess whether or not brain networks participate in a particular process. With MCPA, the two perspectives are merged into one algorithm, which extends multivariate pattern analysis to enable the detailed examination of information sensitivity at the network level. Thus, the introduction of MCPA provides a platform for examining how computation is carried out through the interactions between different brain areas, allowing us to directly test hypotheses regarding circuit-level information processing.

Materials and methods

Overview

The MCPA method consists of a learning phase and a test phase (as in machine learning, where a model is first learned, then tested). In the learning phase, the connectivity maps for each condition that characterize the pattern of shared activity between two populations is learned. In the test phase, these maps are used to generate predictions of the activity in one population based on the activity in the other population as a factor of condition and these predictions are tested against the true activity in the two populations. Similar to linear regression where one can generate a prediction for the single variable A given the single variable B based on the line that correlates A and B, MCPA employs a canonical correlation model (a generalization of multivariate linear regression) and produces a mapping model for each condition as a hyperplane that correlates multidimensional spaces A and B. Thus one can generate a prediction of the observation in multivariate space A given the observation in multivariate space B on a single trials basis. In this sense, MCPA is more analogous to a machine learning classifier combined with a multivariate extension of PPI (21) rather than being analogous to correlation-based functional connectivity measures.

The general framework of MCPA is to learn the connectivity map between the populations for each task or stimulus condition separately based on training data. Specifically, given two neural populations (referred to as A and B), the neural activity of the two populations can be represented by feature vectors in multi-dimensional spaces (14). The actual physical meaning of the vectors would vary depending on modality, for example spike counts for a population of single unit recordings; time point features for

event-related potentials (ERP) or event-related fields; time-frequency features for electroencephalography, electrocorticography (ECoG) or magnetoencephalography; or single voxel blood-oxygen-level dependent (BOLD) responses for functional magnetic resonance imaging. A mapping between A and B is calculated based on any shared information between them for each condition on the training subset of the data. This mapping can be any kind of linear transformation, such as any combination of projections, scalings, rotations, reflections, shears, or squeezes.

These mappings are then tested as to their sensitivity to the differential information being processed between cognitive conditions by determining if the neural activity can be classified based on the mappings. Specifically, for each new test data trial, the maps are used to predict the neural activity in one area based on the activity in the other area and these predictions are compared to the true condition of the data. The trained information-mapping model that fits the data better is selected and the trial is classified into the corresponding condition. This allows one to test whether the mappings were sensitive to the differential information being represented in the neural interaction in the two conditions.

Connectivity Map

The first phase of MCPA is to build the connectivity map between populations. The neural signal in each population can be decomposed into two parts: the part that encodes shared information, and the part that encodes non-shared local information (including any measurement noise). We assume that the parts of the neural activities that represent the shared information in the two populations are linearly correlated (though,

this can easily be extended by the introduction of a non-linear kernel). The model can be described as follows

$$C \sim \mathcal{N}(0, I_d), \min\{m_A, m_B\} \geq d \geq 1$$

$$A|C = W_A C + D, D \sim \mathcal{N}(\mu_A, \Psi_A), W_A \in \mathbb{R}^{m_A \times d}, \Psi_A \succcurlyeq 0$$

$$B|C = W_B C + E, E \sim \mathcal{N}(\mu_B, \Psi_B), W_B \in \mathbb{R}^{m_B \times d}, \Psi_B \succcurlyeq 0$$

where C is the common activity, D and E are local activities, m_A, m_B are the dimensionalities of activity vector in population A and B respectively. Without loss of generality, $\mu_A = \mu_B = 0$ can be assumed. The activity in population A can be decomposed into shared activity $W_A C$ and local activity D, while activity in B can be decomposed into shared activity $W_B C$ and local activity E. The shared discriminant information only lies in the mapping matrix W_A and W_B since C always follows the standard multivariate normal distribution (though correlation measures that do not assume normally distributed data can also be applied with minor modifications to the calculation).

In statistics, canonical correlation analysis (CCA) is optimally designed for such a model and estimate the linear mappings (41, 47). In brief, let S be the covariance matrix

$$S = \begin{bmatrix} S_{AA} & S_{AB} \\ S_{BA} & S_{BB} \end{bmatrix} = \mathbb{E}\left[\begin{pmatrix} A \\ B \end{pmatrix} \begin{pmatrix} A \\ B \end{pmatrix}^T \right]$$

Therefore W_A and W_B can be estimated by solving the following eigen problem

$$\begin{cases} S_{AA}^{-1} S_{AB} S_{BB}^{-1} S_{BA} \widehat{U}_A = \rho^2 \widehat{U}_A \\ S_{BB}^{-1} S_{BA} S_{AA}^{-1} S_{AB} \widehat{U}_B = \rho^2 \widehat{U}_B \end{cases}$$

and we have

$$\begin{cases} \widehat{W}_A = S_{AA} \widehat{U}_{Ad} M_1 \\ \widehat{W}_B = S_{BB} \widehat{U}_{Bd} M_2 \end{cases}$$

where $\widehat{U}_{Ad}$ and $\widehat{U}_{Bd}$ are the first d columns of canonical directions $\widehat{U}_A$ and $\widehat{U}_B$, and M_1, $M_2 \in \mathbb{R}^{d \times d}$ are arbitrary matrices such that $M_1 M_2^T = P_d$, P_d is the diagonal matrix with the first d elements of $P = U_B^T S_{BA} U_A$.

With W_A and W_B, the shared information C can be estimated using its posterior mean $\mathbb{E}(C|A)$ and $\mathbb{E}(C|B)$, where $\mathbb{E}(C|A) = M_1^T U_A^T A$ and $\mathbb{E}(C|B) = M_2^T U_B^T B$. Let $M_1 = M_2$ and equate $\mathbb{E}(C|A)$ and $\mathbb{E}(C|B)$, this shared information can be used as a relay to build the bidirectional mapping between A and B. Specifically, $\widehat{B} = (M_2^T U_B^T)^\dagger M_1^T U_A^T A = U_B^{T\dagger} U_A^T A = RA$ and $\widehat{A} = (M_1^T U_A^T)^\dagger M_2^T U_B^T B = U_A^{T\dagger} U_B^T B = R^\dagger B$, where $R = U_B^{T\dagger} U_A^T A$.

In the first step, the connectivity map is estimated for each condition separately. If we have n_1 trials in condition 1 and n_2 trials in condition 2 in the training set, the training data for the two conditions are represented in matrices as $\left[X_A^{(1)}, X_B^{(1)} \right]^T$ and $\left[X_A^{(2)}, X_B^{(2)} \right]^T$ respectively, where $X_A^{(1)} \in \mathbb{R}^{m_A \times n_1}$, $X_B^{(1)} \in \mathbb{R}^{m_B \times n_1}$ are the population activity for A and B under condition 1 respectively, and $X_A^{(2)} \in \mathbb{R}^{m_A \times n_2}$, $X_B^{(2)} \in \mathbb{R}^{m_B \times n_2}$ are the population activity for A and B under condition 2 respectively. The testing data vector is then represented as $[x_A, x_B]^T$, where $x_A \in \mathbb{R}^{m_A}$ and $x_B \in \mathbb{R}^{m_B}$ are population activities in A and B respectively. Using CCA, the estimations of the mapping matrices with respect to different conditions are $R^{(1)}$ and $R^{(2)}$.

To sum up, by building the connectivity map, a linear mapping function R is estimated from the data for each condition so that the activity of the two populations can be directly linked through bidirectional functional connectivity that captures only the shared information.

Classification

The second phase of MCPA is a pattern classifier that takes in the activity from one population and predicts the activity in a second population based on the learned connectivity maps conditioned upon the stimulus condition or cognitive state. The testing data is classified into the condition to which the corresponding model most accurately predicts the true activity in the second population.

The activity from one population is projected to another using the learned CCA model, i.e. $x_B^{(i)} = U_B^{(i)\dagger} U_A^{(i)} x_A$. The predicted projections $x_B^{(i)}$ are compared to the real observation x_B, and then the testing trial is labeled to the condition where the predicted and real data match most closely. Cosine similarity (correlation) is used as the measurement of the goodness of prediction. The mapping is bidirectional, so A can be projected to B and vice versa. In practice, the similarities from the two directions are averaged in order to find the condition that gives maximum average correlation coefficient.

Simulated experiment

To test the performance of MCPA, we used BOLD signal recorded from areas V1 and V2 to simulate shared and local activity in two populations and tested the performance of MCPA on synthetic data as a factor of the number of dimensions in each population and signal-to-noise ratio (SNR; Figure 2a). In addition to the MVPA control described above, we further evaluated the following three control experiments to demonstrate that MCPA is insensitive to the presence or change in the local information. In the first control experiment (no functional connectivity, no shared information, varying

local information), we used independently sampled random data from area V1 and V2 to

simulated the case where two populations are totally independent under both conditions,

but there is local discriminant information in each (Figure 2b). In the second control

experiment (functional connectivity, constant shared information, varying local

information), we introduced local discriminant information into population A without

changing the amount of shared information between populations A and B (Figure 2c). In

the third control experiment (functional connectivity, no shared information, varying

local information), we eliminated the information represented in the pattern of interaction,

but maintained the functional connectivity by keeping the correlation between

populations invariant with regard to conditions.

For the first simulation (Figure 2a), we sampled from the BOLD signal recorded

from area V1 in the visual cortex and used it as the shared activity, and independently

sampled signal from activity in V1 and V2 as the local unshared activity. (see fMRI

method described below for experiment details). The shared activity for both conditions

in population A was drawn from the first d principal components of V1 activity to mimic

a d-dimensional normal distribution $Y_A^{(i)} \sim \mathcal{N}(0, \Sigma_d)$, for $i = 1,2$, where Σ_d is a diagonal

matrix with the jth element in the diagonal as σ_j^2. The shared activity in population B

under two different conditions were generated by rotating Y_A with different rotation

matrices separately, $Y_B^{(i)} = \mathbf{R}^{(i)} Y_A^{(i)}$, where $\mathbf{R}^{(1)}$ and $\mathbf{R}^{(2)}$ were two d-by-d random

rotation matrices corresponding to the information mapping under condition 1 and 2

respectively, and for simplicity, $\mathbf{R}^{(i)}$ is orthogonal with $\mathbf{R}^{(i)^T}\mathbf{R}^{(i)} = \mathbf{I}_d$. In addition to the

shared activity, local activity in A and B was randomly drawn from the first d principal

components of V1 and V2 activity respectively and multiplied by a factor of σ to

simulate white noise $\boldsymbol{E}^{(i)} \sim \mathcal{N}(0, \sigma^2 \boldsymbol{\Sigma}_d)$.

The two important parameters here are the dimensionality d and the variance σ^2.

SNR was used to characterize the ratio between the variance of shared activity and

variance of local activity, and the logarithmic decibel scale $\text{SNR}_{dB} = -10 \log_{10}(\sigma^2)$ was

used. To cover the wide range of possible data recorded from different brain regions and

different measurement modalities, we tested the performance of MCPA with d ranging

from 2 to 25 and SNR ranging from -20 dB to 20 dB (σ^2 ranged from 0.01 to 100). Note

that each of the d dimensions contain independent information about the conditions

though have the same SNR. Thus the overall SNR does not change, but the amount of

pooled information does change with d. For each particular setup of parameters, the

rotation matrices $\mathbf{R}^{(i)}$ were randomly generated first, then 200 trials were randomly

sampled for each condition and evenly split into training set and testing set. MCPA was

trained using the training set and tested on the testing set to estimate the corresponding

true positive rate (TPR) and false positive rate (FPR) for the binary classification. The

sensitivity index d' was then calculated as $d' = Z(TPR) - Z(FPR)$, where $Z(x)$ is the

inverse function of the cdf of standard normal distribution. This process was repeated 100

times and the mean and standard errors across these 100 simulations were calculated.

Note that the only discriminant information about the two conditions is the pattern of

interactions between the two populations, and neither of the two populations contains

local discriminant information about the two conditions in its own activity. We further

tested and confirmed this by trying to classify the local activity in populations A and B

(see below). To avoid an infinity d' value, with 100 testing trials, the maximum and

minimum for TPR or FRP were set to be 0.99 and 0.01, which made the maximum possible *d'* to be 4.65.

The MCPA method captures the pattern of correlation between neural activities from populations and is invariant to the discriminant information encoded in local covariance. To see this, we first take the simulation data described above and apply MVPA (naïve Bayes) to each of the two populations separately. Note that in each of the two populations, we set the two conditions to have the same mean and covariance. As a result, there should be no local discriminant information within any of the two populations alone.

Control simulations

For the first control simulation (Figure 2b), for condition 1, $X_A^{(1)}, X_B^{(1)}$ were drawn independently from the first *d* principal components of area V1 and area V2; for condition 2, $X_A^{(2)}, X_B^{(2)}$ were drawn independently from the same distribution in the first *d* principal components of area V1 and area V2. Then we changed the local variance in one of the conditions. For the features in population A and B under condition 1, we used $X_A^{(1)'} = kX_A^{(1)}$ and $X_B^{(1)'} = kX_B^{(1)}$, where *k* ranged from 1 to 9. Thus, in both populations, the variance of condition 1 was different from the variance of condition 2, and such difference would increase as *k* became larger. Therefore, there was no information shared between the two populations under either condition, but each of the population had discriminant information about the conditions encoded in the variance for any $k \neq 1$.

For the second control simulation (Figure 2c), we fixed the dimensionality at 10 and SNR at 0 dB ($\sigma^2 = 1$) and kept the rotation matrices of different conditions different

from each other. As a result, the amount of shared discriminant information represented in the patterns of interactions stayed constant. Then we changed the local variance in one of the conditions. For the features in population A under condition 1, we used $X_A^{(1)'} = kX_A^{(1)}$, where k ranged from 1 to 9. Thus, population A, the variance of condition 1 was different from the variance of condition 2, and such difference would increase as k became larger. According to our construction of MCPA, it should only pick up the discriminant information contained in the interactions and should be insensitive to the changes in local discriminant information from any of the two populations.

For the third control simulation (Figure 2d), we introduced local discriminant information into the two populations to demonstrate that MCPA is insensitive to the presence of constantly correlated local information (figure 2d). We fixed the dimensionality at 10 and SNR at 0 dB ($\sigma^2 = 1$) and kept the rotation matrices constant for different conditions. As a result, the amount of shared discriminant information represented in the patterns of interactions was 0. Then we changed the local variance in one of the conditions. Then we changed the local variance in one of the conditions. For the features in population A and B under condition 1, we used $X_A^{(1)'} = kX_A^{(1)}$ and $X_B^{(1)'} = kX_B^{(1)}$, where k ranged from 1 to 9. Thus, in both populations, the variance of condition 1 was different from the variance of condition 2, and such difference would increase as k became larger. Notably, such local information was actually correlated through interactions between the populations. However, since the pattern of interaction did not vary as the condition changed, there was no discriminant information about the conditions represented in the interactions. According to our construction of MCPA, it should not pick up any discriminant information in this control case.

Examining visual cortex coding for natural images using MCPA

fMRI methods

The fMRI dataset was taken from CRCNS.org (30). See (29, 31) for details regarding subjects, stimuli, MRI parameters, data collection, and data preprocessing. In the experiment, two subjects performed passive natural image viewing tasks while BOLD signals were recorded from the brain. The experiment contains two stages: a training stage and a validation stage. In the training stage, two separate trials were recorded in each subject. In each trial, a total of 1750 images were presented to the subject, which yields a total of 3500 presentations of images (3500 = 1750 images * 2 repeats). In the validation stage, another 120 images were presented to the subject in 13 repeated trials, which yields a total of 1560 presentations (1560 = 120 images * 13 repeats). The single-trial response for each voxel was estimated using deconvolution method and used for the following analysis. The voxels were assigned to 5 visual areas (V1, V2, V3, V4, and LO) based on retinotopic mapping data from separate scans (29, 31).

Categorical image classification

To control for repetition of each individual image and increase the image number being used, we used the data from the training stage for the categorical image classification. The 1750 images were manually sorted into 8 categories (animals, buildings, humans, natural scenes, textures, food, indoor scenes, and manmade objects). In order to maintain enough statistical power, only categories with more than 100 images

were used in the analysis. As a result, 3 categories (food, indoor scenes, and manmade objects) were excluded.

For each pair of ROIs, namely V1-V2, V2-V3, V3-V4, and V4-LO, MCPA was applied to classify the functional connectivity patterns for each possible pair of image categories (total of 10 pairs). For each specific pair of categories, BOLD signal from all the voxels in the ROIs were used as features in MCPA. Principal Component Analysis (PCA) was used to reduce the dimensionality to P, where P corresponds to the number of PCs that capture 90% of variation in the data, which yielded between 100-200 PCs. Leave-one-trial-out cross-validation was used in order to estimate the classification accuracy. This procedure was repeated for all 10 pairs. *d'* was used to quantify the performance of MCPA.

Single image classification using MCPA

For single image classification the 13 repetitions of each individual image from the validation stage data was used.

For each pair of ROIs, namely V1-V2, V2-V3, V3-V4, and V4-LO, MCPA was applied to classify the functional connectivity patterns for each possible pair of images (total of 7140 pairs). For each specific pair of categories, BOLD signal from all the voxels in the ROIs were used as features in MCPA. Considering the limited number of trials in each condition, PCA was first used with the data from the training stage to reduce the representation dimensionality to 10. Because the top PCs that explain most variations may contain variance not related to the stimuli, the 10 PCs were selected from the top 50 PCs, based on maximizing the between-trial correlations for single images. As

a result, we reduced the dimensionality of the validation data from more than 1000 to 10

based on the training dataset, which was completely independent from all the validation

data that was used in the learning and testing stages of MCPA. Leave-one-trial-out cross-

validation was then used in order to estimate the classification accuracy. This procedure

was repeated for all 7140 pairs. *d'* was used to quantify the performance of MCPA.

MVPA analysis

MVPA was applied to classify the neural activity within each ROI (V1, V2, V3,

V4, and LO) for each possible pair of categories (total of 10 pairs). The same features

extracted from all the voxels within the ROI, as described above, were used in MVPA

analysis. Naïve Bayes classifier was used as the linear classifier and leave-one-trial-out

cross-validation was used in order to estimate the classification accuracy. This procedure

was repeated for all 10 pairs. *d'* was used to quantify the performance of MVPA.

Permutation test

Permutation testing was used to determine the significance of the classification

accuracy *d'*. For each permutation, the condition labels of all the trials were randomly

permuted and the same procedure as described above was used to calculate the *d'* for

each permutation. The permutation was repeated for a total of 200 times. The *d'* of each

permutation was used as the test statistic and the null distribution of the test statistic was

estimated using the histogram of the permutation test.

Representational similarity analysis

Based on the classification results, for each classification analysis, the representational dissimilarity matrix (RDM) **M** was constructed such that the *j*th element in the *i*th row, m_{ij} , equals the dissimilarity (classification accuracy) between the condition *i* and condition *j* in the corresponding representational space defined by the analysis. Spearman's rank correlation was used to compare representational dissimilarity matrices in order to account for outliers and non-normality in the data.

Psychophysiological interactions

PPI (21) was used to analyze the pattern of interactions between V1 and V4 for each pair of image categories (total of 10). The response in each ROI was extracted by taking the first principal component across all voxels. The PPI model can be written as $y = \beta_1 x_1 + \beta_2 x_2 + \beta_3 x_3 + \epsilon$, where *y* is the response in V4, x_1 is the response in V1, x_2 is the categorical condition (1 or -1), and x_3 is the psychophysiological interaction ($x_3 = x_1 \cdot x_2$).

HMAX model and connectivity patterns

The implementation of HMAX model by Serre et al. (33) was used. Each image was fed into the network and the activations in the four layers (S1, C1, S2, and C2) were recorded. At each patch size level, for image *k* (*k* = 1, 2, …, 120), the activation pattern in simple layer *i* (*i* = 1, 2) is recorded as $\mathbf{S}_i^k$, which is a square matrix with retinotopic mapping to the image space. On the other hand, the activation pattern in complex layer *i* (*i* = 1, 2) is represented as vector C_i^k with each element representing the activation of one single unit (for C1, this is achieved by concatenating all the units in the layer into one

vector). The activation of each unit in the complex layer was calculated by taking a

maximum over its corresponding pool of units in the previous simple layer. For each

complex unit, we recorded the location of the corresponding maximum activation simple

unit. As a result, we got a N_i-by-2 connectivity matrix $\mathbf{V}_i^k$ for complex layer Ci for image

k, where N_i is the total number of units in Ci and each row is the 2-D coordinate of the

corresponding maximum activation simple unit. Thus, the connectivity pattern between

simple layer Si and complex layer Ci for image k was described by such connectivity

matrix $\mathbf{V}_i^k$. Considering all pairs of images, the RDM of the connectivity pattern $\mathbf{M}_i$ is

calculated by taking the Frobenius norm of the difference between each pair of

connectivity matrix, i.e. $\mathbf{M}_i(j, k) = \left\| \mathbf{V}_i^j - \mathbf{V}_i^k \right\|_2$.

The representation space for each single layer was then extracted by

concatenating all units in the layer into one vector. The RDM of each single layer was

calculated using the Euclidian distance between the corresponding activation vectors of

the images.

Representational similarity analysis and permutation test

Permutation test was used to determine the statistical significance of the

correlation between the RDM from MCPA and the RDM from HMAX. Specifically, for

each pair of ROIs (i.e. V1-V2, V2-V3, V3-V4, and V4-LO), we calculated the

corresponding 120-by-120 RDM for all the images from MCPA and averaged across the

two subjects, noted as $\mathbf{M}^{ROI1-ROI2}$, where $ROI1$-$ROI2$ = V1-V2, V2-V3, V3-V4, or V4-

LO. Then we used the RDMs of HMAX ($\mathbf{M}_i$, i = 1, 2) described in the previous part and

calculate the Spearman's rank correlation between $\mathbf{M}^{ROI1-ROI2}$ and $\mathbf{M}_i$. As a result, we

have $\rho_i^{ROI1-ROI2} = corr(\mathbf{M}^{ROI1-ROI2}, \mathbf{M}_i)$. Then to compare the correlation from

different layers in HMAX to MCPA, we use $\Delta\rho^{ROI1-ROI2} = \rho_1^{ROI1-ROI2} - \rho_2^{ROI1-ROI2}$ as

the test statistic. For each permutation, the labels of the 120 images were randomly

permuted and the above procedure was repeated. With a total of 500 permutations, we got

the empirical distribution of the test statistic for the null hypothesis that there is no

difference between the two correlations. A p-value for the real test statistic can then be

estimated.

Acknowledgements

Reference:

1.   Hubel DH & Wiesel TN (1959) Receptive Fields of Single Neurones in the Cats Striate Cortex. *J Physiol-London* 148(3):574-591.

2.   Desimone R, Albright TD, Gross CG, & Bruce C (1984) Stimulus-selective properties of inferior temporal neurons in the macaque. *J Neurosci* 4(8):2051-2062.

3.   Tsao DY, Freiwald WA, Tootell RB, & Livingstone MS (2006) A cortical region consisting entirely of face-selective cells. *Science* 311(5761):670-674.

4.   Haxby JV, *et al.* (2001) Distributed and overlapping representations of faces and objects in ventral temporal cortex. *Science* 293(5539):2425-2430.

5.   Cox DD & Savoy RL (2003) Functional magnetic resonance imaging (fMRI) "brain reading": detecting and classifying distributed patterns of fMRI activity in human visual cortex. *Neuroimage* 19(2 Pt 1):261-270.

6.   Kamitani Y & Tong F (2005) Decoding the visual and subjective contents of the human brain. *Nat Neurosci* 8(5):679-685.

7.   Polyn SM, Natu VS, Cohen JD, & Norman KA (2005) Category-specific cortical activity precedes retrieval during memory search. *Science* 310(5756):1963-1966.

8.   Haynes JD & Rees G (2006) Decoding mental states from brain activity in humans. *Nature Reviews Neuroscience* 7(7):523-534.

9.   Poldrack RA (2011) Inferring mental states from neuroimaging data: from reverse inference to large-scale decoding. *Neuron* 72(5):692-697.

10.   Ghuman AS, *et al.* (2014) Dynamic encoding of face information in the human fusiform gyrus. *Nat Commun* 5:5672.

11.   Hirshorn EA*, et al.* (2016) Decoding and disrupting left midfusiform gyrus activity during word reading. *Proc Natl Acad Sci U S A* 113(29):8162-8167.

12.   Edelman S, Grill-Spector K, Kushnir T, & Malach R (1998) Toward direct visualization of the internal shape representation space by fMRI. *Psychobiology* 26(4):309-321.

13.   Kriegeskorte N & Kievit RA (2013) Representational geometry: integrating cognition, computation, and the brain. *Trends Cogn Sci* 17(8):401-412.

14.   Haxby JV, Connolly AC, & Guntupalli JS (2014) Decoding Neural Representational Spaces Using Multivariate Pattern Analysis. *Annu Rev Neurosci* 37:435-456.

15.   Grossberg S (1980) How Does a Brain Build a Cognitive Code. *Psychol Rev* 87(1):1-51.

16.   Lee TS & Mumford D (2003) Hierarchical Bayesian inference in the visual cortex. *J Opt Soc Am A* 20(7):1434-1448.

17.   Kveraga K, Ghuman AS, & Bar M (2007) Top-down predictions in the cognitive brain. *Brain Cogn* 65(2):145-168.

18.   Freiwald WA, Tsao DY, & Livingstone MS (2009) A face feature space in the macaque temporal lobe. *Nat Neurosci* 12(9):1187-1196.

19.   Nestor A, Plaut DC, & Behrmann M (2011) Unraveling the distributed neural code of facial identity through spatiotemporal pattern analysis. *P Natl Acad Sci USA* 108(24):9998-10003.

20.   Fodor JA (1983) *The modularity of mind : an essay on faculty psychology* (MIT Press, Cambridge, Mass.) p 145 p.

21. Friston KJ*, et al.* (1997) Psychophysiological and modulatory interactions in neuroimaging. *Neuroimage* 6(3):218-229.

22. Friston KJ, Harrison L, & Penny W (2003) Dynamic causal modelling. *Neuroimage* 19(4):1273-1302.

23. Norman KA, Polyn SM, Detre GJ, & Haxby JV (2006) Beyond mind-reading: multi-voxel pattern analysis of fMRI data. *Trends Cogn Sci* 10(9):424-430.

24. Wang YD, Cohen JD, Li K, & Turk-Browne NB (2015) Full correlation matrix analysis (FCMA): An unbiased method for task-related functional connectivity. *J Neurosci Meth* 251:108-119.

25. Cribben I, Haraldsdottir R, Atlas LY, Wager TD, & Lindquist MA (2012) Dynamic connectivity regression: determining state-related changes in brain connectivity. *Neuroimage* 61(4):907-920.

26. Finn ES*, et al.* (2015) Functional connectome fingerprinting: identifying individuals using patterns of brain connectivity. *Nat Neurosci* 18(11):1664-1671.

27. Richiardi J, Eryilmaz H, Schwartz S, Vuilleumier P, & Van De Ville D (2011) Decoding brain states from fMRI connectivity graphs. *Neuroimage* 56(2):616-626.

28. Shirer WR, Ryali S, Rykhlevskaia E, Menon V, & Greicius MD (2012) Decoding subject-driven cognitive states with whole-brain connectivity patterns. *Cereb Cortex* 22(1):158-165.

29. Kay KN, Naselaris T, Prenger RJ, & Gallant JL (2008) Identifying natural images from human brain activity. *Nature* 452(7185):352-355.

30.   Kay KN, Naselaris T, & Gallant JL (2011) fMRI of human visual areas in response to natural images. (CRCNS.org).

31.   Naselaris T, Prenger RJ, Kay KN, Oliver M, & Gallant JL (2009) Bayesian reconstruction of natural images from human brain activity. *Neuron* 63(6):902-915.

32.   Riesenhuber M & Poggio T (1999) Hierarchical models of object recognition in cortex. *Nat Neurosci* 2(11):1019-1025.

33.   Serre T, Wolf L, Bileschi S, Riesenhuber M, & Poggio T (2007) Robust object recognition with cortex-like mechanisms. *IEEE Trans Pattern Anal Mach Intell* 29(3):411-426.

34.   Gilbert CD & Li W (2013) Top-down influences on visual processing. *Nat Rev Neurosci* 14(5):350-363.

35.   Kriegeskorte N (2011) Pattern-information analysis: From stimulus decoding to computational-model testing. *Neuroimage* 56(2):411-421.

36.   Kriegeskorte N, Mur M, & Bandettini P (2008) Representational similarity analysis - connecting the branches of systems neuroscience. *Front Syst Neurosci* 2:4.

37.   Rosenberg MD*, et al.* (2016) A neuromarker of sustained attention from whole-brain functional connectivity. *Nat Neurosci* 19(1):165-171.

38.   Coutanche MN & Thompson-Schill SL (2013) Informational connectivity: identifying synchronized discriminability of multi-voxel patterns across the brain. *Front Hum Neurosci* 7:15.

39.   O'Reilly JX, Woolrich MW, Behrens TE, Smith SM, & Johansen-Berg H (2012) Tools of the trade: psychophysiological interactions and functional connectivity. *Soc Cogn Affect Neurosci* 7(5):604-609.

40.   Yamins DL*, et al.* (2014) Performance-optimized hierarchical models predict neural responses in higher visual cortex. *Proc Natl Acad Sci U S A* 111(23):8619-8624.

41.   Hardoon DR, Szedmak S, & Shawe-Taylor J (2004) Canonical correlation analysis: an overview with application to learning methods. *Neural Comput* 16(12):2639-2664.

42.   Andrew G, Arora R, Bilmes J, & Livescu K (2013) Deep Canonical Correlation Analysis. *The 30th International Conference on Machine Learning*, (JMLR W&CP), pp 1247-1255.

43.   Kettenri.Jr (1971) Canonical Analysis of Several Sets of Variables. *Biometrika* 58(3):433-&.

44.   Kriegeskorte N, Goebel R, & Bandettini P (2006) Information-based functional brain mapping. *P Natl Acad Sci USA* 103(10):3863-3868.

45.   Rumelhart DE, Hinton GE, & Williams RJ (1986) Learning Representations by Back-Propagating Errors. *Nature* 323(6088):533-536.

46.   Friston K (2010) The free-energy principle: a unified brain theory? *Nat Rev Neurosci* 11(2):127-138.

47.   Bach FR & Jordan MI (2005) A probabilistic interpretation of canonical correlation analysis. (Technical Report 688, Department of Statistics, University of California, Berkeley).
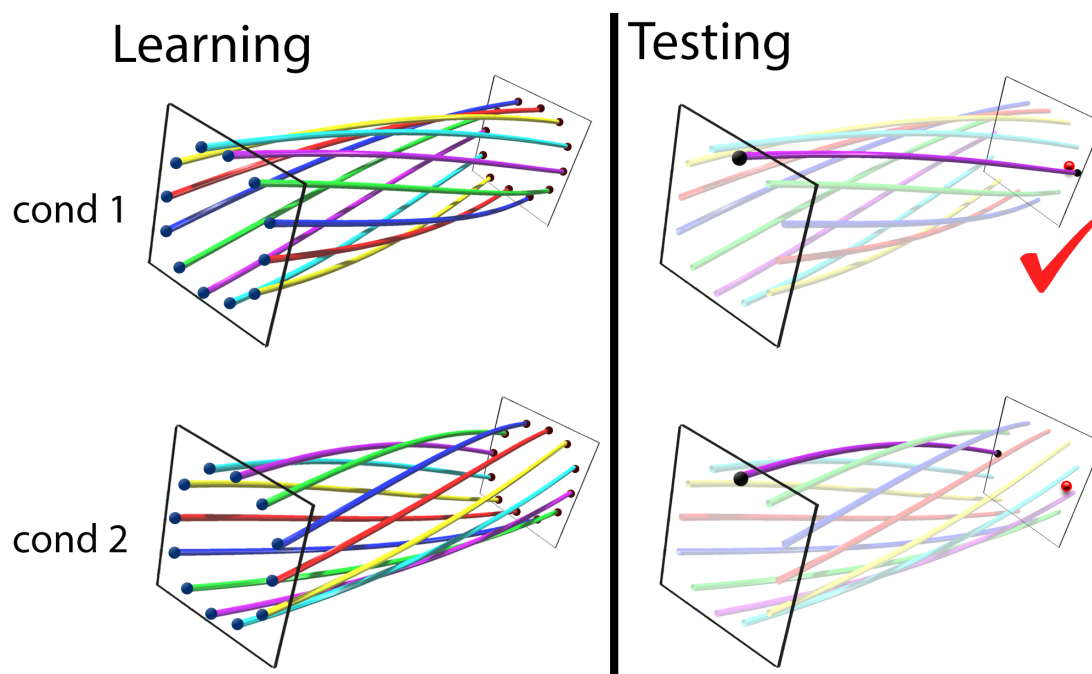
Figure 1. Illustration of the connectivity map and classifier of MCPA.

The MCPA framework is demonstrated as a two-phase process: learning and testing.

Top left: An illustration of the learned functional information mapping between two populations under condition 1. The representational state spaces of the two populations are shown as two planes and each pair of blue and red dots correspond to an observed data point from the populations. The functional information mapping is demonstrated as the colored pipes that project points from one space onto another (in this case, a 90 degree clockwise rotation).

Bottom left: An illustration of the learned functional information mapping between two populations under condition 2 (in this case, a 90 degree counterclockwise rotation).

Top right: An illustration of the predicted signal by mapping the observed neural activity from one population onto another using the mapping patterns learned from condition 1. The real signal in the second population is shown by the red dot.

Bottom right: An illustration of the predicted signal by mapping the observed neural activity from one population onto another using the mapping patterns learned from condition 2.

In this case, MCPA would classify the activity as arising from condition 1 because of the better match between the predicted and real signal.
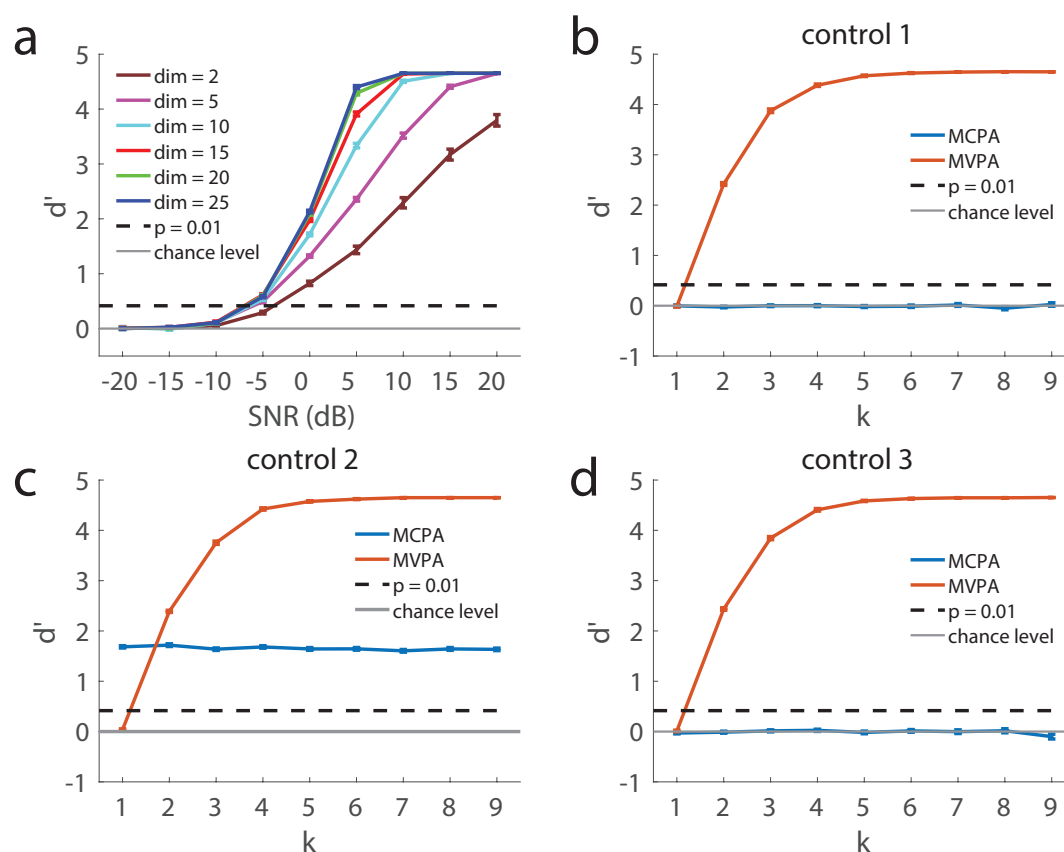
Figure 2. Synthetic data and control simulation experiments. The mean and standard error for 100 simulation runs are plotted. The horizontal gray line corresponds to chance level ($d' = 0$). The dashed line ($d' = 0.42$) corresponds to the chance threshold, $p = 0.01$, based on a permutation test. The maximum possible $d' = 4.65$ (equivalent to 99% accuracy because the d' for 100% accuracy is infinity).

a) The sensitivity of MCPA for connectivity between two populations as a factor of SNR and the number of effective dimensions in each population. MCPA was applied to synthetic data, where two conditions had different patterns of functional connectivity (measured by SNR and dimensionality). Performance of MCPA was significantly higher than chance level when SNR $\geq$ -5 dB and the number of dimensions $\geq$ 2. Performance of MCPA saturated to maximum when SNR > 5 dB and the number of dimensions > 10.

b) The insensitivity of MCPA when there is variable local discriminant information, but no circuit-level information (control case 1). MCPA and MVPA were applied to control case 1. The SNR was fixed at 0 dB and the number of dimensions is fixed at 10 for panels b, c, and d. k corresponds to the ratio of the standard deviations of the two conditions in panels b, c, and d.

c) The insensitivity of MCPA to changes in local discriminant information with fixed circuit-level information when there is both local and circuit-level information (control case 2).

d) The insensitivity of MCPA to variable local discriminant information when the circuit-level activity is correlated, but does not contain circuit-level information about what is being processed (control case 3).
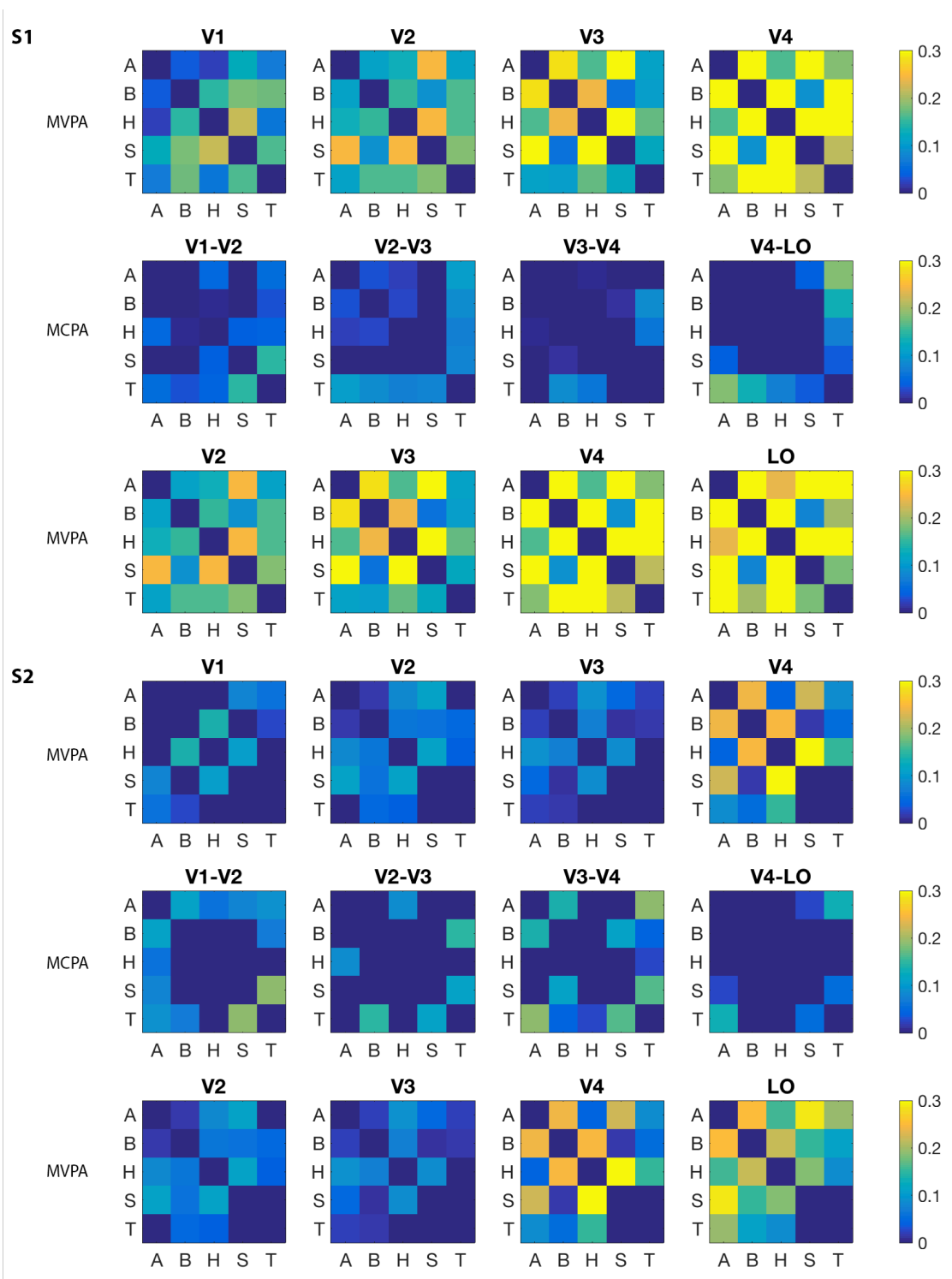
Figure 3. MCPA and MVPA results for fMRI categorical data.

RSA results based on MCPA and MVPA for V1, V2, V3, V4, and LO from Subjects 1 and 2. Categories: A-animals, B-buildings, H-humans, S-natural scenes, T-textures.

Row 1 & 3: RSA based on MVPA for V1, V2, V3, V4, and LO of Subject 1, each entry represents the classification accuracy (d') between the corresponding categories;

Row 2: RSA based on MCPA for V1-V2, V2-V3, V3-V4, and V4-LO of Subject 1, each entry represents the classification accuracy (d') between the corresponding categories;

Row 4 & 6: RSA based on MVPA for V1, V2, V3, V4, and LO of Subject 2, each entry represents the classification accuracy (d') between the corresponding categories;

Row 5: RSA based on MCPA for V1-V2, V2-V3, V3-V4, and V4-LO of Subject 2, each entry represents the classification accuracy (d') between the corresponding categories.
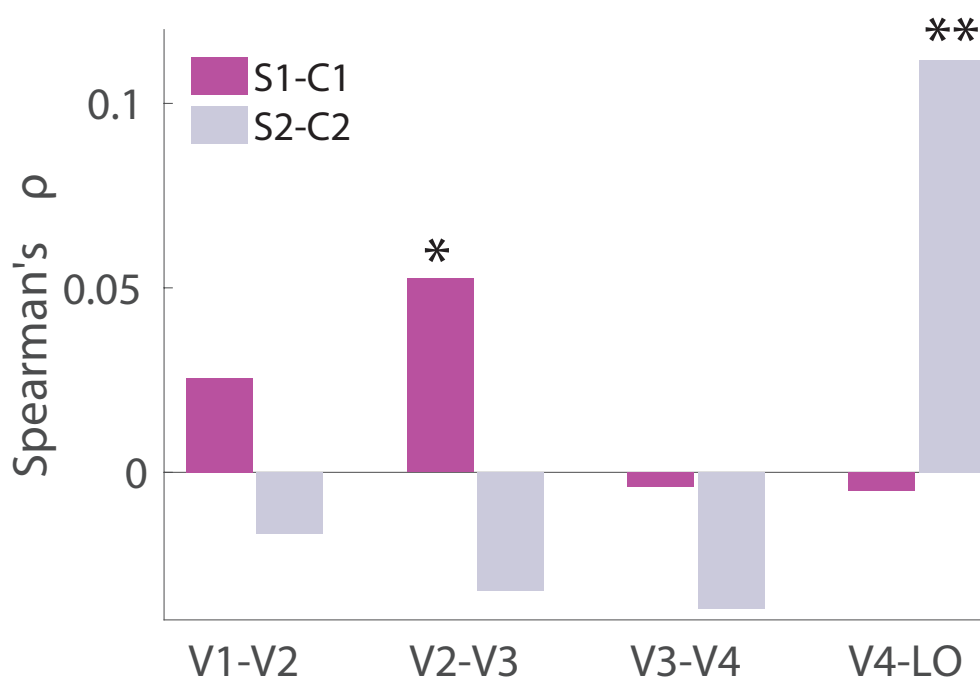
Figure 4. Correlating MCPA and HMAX. Correlation coefficients between the between-layer connectivity patterns in HMAX (S1-C1, and S2-C2) and the between-area connectivity patterns in fMRI data extracted by MCPA (V1-V2, V2-V3, V3-V4, and V4-LO) were plotted. The correlation was evaluated by Spearman's rank correlation coefficients. For S1-C1, correlation peaked at V2-V3, mean Spearman's rho = 0.053 (* p = 0.036, permutation test within each subject, and p-values were combined using Fisher's method). For S2-C2, correlation peaked at V4-LO, mean Spearman's rho = 0.112 (** p < 0.001, permutation test within each subject, and p-values were combined using Fisher's method).

Table 1 Spearman's rank correlation coefficients between MCPA of ROI1-ROI2 and MVPA of ROI1 or ROI2 in Subjects 1 and 2.

Subject 1				
ROI1-ROI2	V1-V2	V2-V3	V3-V4	V4-LO
ROI1	0.333	-0.055	-0.721	-0.442
ROI2	0.176	-0.370	-0.491	-0.442
Subject 2				
ROI1-ROI2	V1-V2	V2-V3	V3-V4	V4-LO
ROI1	-0.539	-0.758	-0.782	-0.539
ROI2	-0.855	-0.794	-0.418	0.055